ISSN 0026-8933, Molecular Biology, 2016, Vol. 50, No. 6, pp. 812–822. © Pleiades Publishing, Inc., 2016.
Original Russian Text © O.I. Volokh, N.I. Derkacheva, V.M. Studitsky, O.S. Sokolova, 2016, published in Molekulyarnaya Biologiya, 2016, Vol. 50, No. 6, pp. 922–934.

REVIEWS

UDC 615.277.3;577.214.39

Structural Studies of Chromatin Remodeling Factors

O. I. Volokh[a], N. I. Derkacheva[b], V. M. Studitsky[a, c], and O. S. Sokolova[a, *]

[a] *Biological Faculty, Moscow State University, Moscow, 119234 Russia;*
[b] *Biochemistry Department, Evdokimov University of Medicine and Dentistry, Moscow, 127473 Russia*
[c] *Fox Chase Cancer Center, Philadelphia, PA, 19111 USA*
**e-mail: sokolova184@gmail.com*

Received March 17, 2016; in final form, March 24, 2016

Abstract—Changes of chromatin structure require participation of chromatin remodeling factors (CRFs), which are ATP-dependent multisubunit complexes that change the structure of the nucleosome without covalently modifying its components. CRFs act together with other protein factors to regulate the extent of chromatin condensation. Four CRF families are currently distinguished based on their structural and biochemical characteristics: SWI/SNF, ISWI, Mi-2/CHD, and SWR/INO80. X-ray diffraction analysis and electron microscopy are the main methods to obtain structural information about macromolecules. CRFs are difficult to obtain in crystal because of their large sizes and structural heterogeneity, and transmission electron microscopy (TEM) is mostly employed in their structural studies. The review considers all structures obtained for CRFs by TEM and discusses several models of CRF–nucleosome interactions.

Keywords: chromatin remodeling factors, transmission electron microscopy, chromatin, transcription, nucleosome
DOI: 10.1134/S0026893316060212

INTRODUCTION

Nuclear DNA occurs in complex with histones and nonhistone proteins to form chromatin in eukaryotic cells. Histones provide for DNA supercoiling and condensation, and chromatin is involved in replication, transcription, repair, and recombination. A nucleosome is a main structural unit of chromatin and consists of a 147-bp DNA segment wrapped around an octamer of histones H2A, H2B, H3, and H4. A linker DNA segment between nucleosomes is approximately 60 bp on average. This DNA segment interacts with linker histone H1. Alternative variants that may be incorporated in nucleosomes are known for all but one histone, H4. Nucleosomal histones can additionally undergo covalent modification, including acetylation, methylation, phosphorylation, etc. Processes associated with changes in histone composition (histone exchange) or conformation play an important role in controlling gene expression, establishing epigenetic memory, and regulating DNA repair. Chromatin reorganization and nucleosome assembly and disassembly accompany all processes that occur in the cell and involve its genetic material. Changes in the nucleosomal composition of chromatin require specific protein complexes that are known as chromatin remodeling factors (CRFs) [1–5].

Abbreviations: CRF, chromatin remodeling factor; RCT, random conical tilt; TEM, transmission electron microscopy; 3D, three-dimensional; 2D, two-dimensional; NS, negative staining; STEM, scanning TEM.

CRFs are ATP-dependent multisubunit complexes that noncovalently change the nucleosome structure. All CRFs have a core catalytic subunit with an ATPase domain, which belongs to DNA helicase superfamily 2 (SF2, or SNF2). CRFs utilize the energy of ATP hydrolysis to change the chromatin packaging pattern by moving, destabilizing, or restructuring nucleosomes or partly or completely removing histone complexes from DNA [1, 6, 7]. CRFs act together with other protein factors to regulate the extent of chromatin condensation; this effect is essential for modulating the accessibility of particular DNA regions (enhancers, promoters, and origins of replication) to regulatory proteins in the course of DNA transcription, replication, repair, and recombination. DNA accessibility is possible to change by shifting nucleosomes, removing them partly or completely, or unwinding a DNA segment from the histone octamer.

Almost all processes that involve chromatin DNA require CRFs. First, specialized CRFs ensure a correct nucleosome distribution along DNA after replication. Second, CRFs are necessary for transcription, replication, and their regulation. CRFs function to open important cis-regulatory DNA elements inaccessible because of a compact nucleosome packaging. In addition, CRFs are essential for replication elongation and transcription. As DNA and RNA polymerases progress along DNA, template regions are released from nucleosomes, which form again on DNA afterwards. Specialized CRFs facilitate the poly-

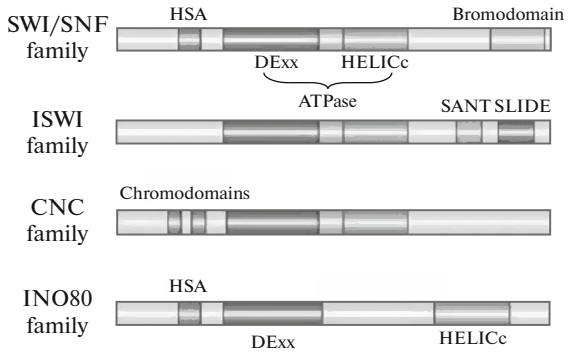

Fig. 1. Domain structure of the ATPase subunit in CRFs of different families (cited from [1]).

merase progress. CRFs can occupy nucleosome-free DNA regions. Third, specialized CRFs ensure nucleosome mobility during recombination and repair and release DNA segments to allow their interactions with corresponding enzymes.

All CRFs have several properties in common:

• their affinity for nucleosomes is higher than for DNA;

• they have domains capable of recognizing covalent histone modifications;

• they possess a DNA-dependent ATPase domain, which works as a DNA translocation motor and disrupts the DNA–histone interaction;

• they have domains or subunits that regulate the ATPase domain; and

• they have domains or subunits that interact with other chromatin or transcription factors.

Four CRF families are currently recognized based on their structural and biochemical features: SWI/SNF, ISWI, Mi-2/CHD, and SWR/INO80. The catalytic subunits of all CRFs have a conserved ATPase domain, but differ by the presence or absence of other additional domains (Fig. 1).

The ATPase domain consists of two parts, DExx and HELICc, which are close together in members of the SWI/SNF, ISWI, and Mi-2/CHD families and far apart in members of the SWR/INO80 family. The SWI/SNF family is characterized by the presence of a bromodomain, which consists of approximately 110 amino acid residues and specifically binds to the ε-acetylamino groups of lysine residues in histones. A helicase/SANT-associated (HAS) domain occurs at the N end of SWI/SNF and SWR/INO80 family CRFs. The HAS domain is presumably involved in DNA binding. Members of the ISWI family have a SANT-SLIDE domain, which is involved in histone binding. A tandem of chromodomains, which recognized methylated lysine residues in histones, is characteristic of Mi-2/CHD family members.

SPECIFICS OF STRUCTURAL STUDIES WITH CRFs

The three-dimensional (3D) structures of CRFs are difficult to examine. First, higher eukaryotic CRFs form multisubunit complexes with a molecular mass ranging from 300 kDa to 1.5 MDa [1, 8]. Second, CRFs may have 1 to 15 different subunits. Finally, CRF assembly in vitro is problematic, requiring that native samples be isolated from eukaryotic cells. In spite of intense research, the mechanisms of action of various CRFs are still a matter of discussion, in particular, as a result of CRF diversity. Structural characteristics of single CRFs and their complexes with nucleosomes may shed light on the functional specifics of different CRF families.

X-ray diffraction analysis and electron microscopy are the main methods that are used to obtain structural information for macromolecules. X-ray quality crystals of CRFs are difficult to obtain because of their large sizes and heterogeneity. Crystal structures are available now only for individual domains of several CRFs, and transmission electron microscopy (TEM) is therefore the method of choice. TEM requires small amounts of samples and yields information on the 3D sample structure, which can then be refined using X-ray diffraction data on particular CRF components.

Electron microscopy of macromolecules provides a potent tool to visualize their structural details. The 3D structure of a molecule is possible to reconstruct because purified molecular complexes occur in the form of isolated particles and usually vary in orientation in a sample. An electron micrograph contains a set of two-dimensional (2D) projections of 3D entities. To establish the original structure, multiples views of a specimen should be aligned and collated.

Almost all structures assumed for CRFs to date are based on TEM of macromolecules (table).

Building a primary model is a critical step in 3D reconstruction. There are several circumstances that make it rather difficult to obtain a high-quality 3D structure for CRFs:

• complexes lack symmetry in the majority of cases;

• complexes have high conformational mobility;

• samples are heterogeneous; and

• stable CRF–nucleosome complexes are difficult to obtain in sufficient amounts.

The role of these circumstances in 3D reconstructions of several CRFs is considered below.

Electron Microscopy with Negative Staining of Samples

Negative staining is the simplest means to study the structures of macromolecular complexes in a solution or a suspension of isolated macromolecules with a low (<0.1 mg/mL) concentration. A sample applied on a grid is treated with an aqueous solution of a heavy

CRF families and their members with TEM structures determined partly or completely

Family	CRF with a 3D structure described	Method used to obtain the structure	Maximal resolution, Å
SWI/SNF	RSC [9–12] PBAF [13] SWI/SNF [14, 15]	NS*, Cryo-EM NS NS, Cryo-EM	25 43 23
ISWI	CHRAC [16] ACF [17] ISW1a-Δ ATPase [18]	NS NS Cryo-EM	27 27 22
Mi-2/CHD	None	–	–
SWR/INO80	INO80 [19] SWR1 [20]	NS Cryo-EM	17.5 28

*NS, negative staining with heavy metal salts.

metal salt (usually 1–2% uranyl acetate), excess fluid is removed, and the sample is dried [21]. Uranyl acetate is the most common stain and produces a high image contrast, but certain protein structures are better preserved with other contrast agents, such as tungsten or molybdenum salts [21, 22]. A contrast agent forms an electron-dense coating on the surface of the sample under study and thus makes it possible to obtain information on the sizes, shapes, and symmetry of protein particles and to evaluate the sample homogeneity. The method is termed negative staining because macromolecules are seen as light stain-free areas. Some molecules are well preserved upon negative staining, while complexes may slightly collapse or decompose upon staining or subsequent air drying. When the orientation of molecules on a grid is constant rather than random, a random conical tilt (RCT) procedure is employed [9, 11]. In this case, two images are taken of the same set of particles on the grid at different tilts (e.g., 0° and 50°).

Negative contrasting was used to reconstruct the structures of RSC [9–12], PBAF [13], SWI/SNF [14], CHRAC [16], ACF [17], and INO80 [19] (Figs. 2–4).

RSC Complex

TEM data on the structure of a negatively stained RSC complex illustrate the above problems. Two of the four TEM structures published for the RSC complex to date were obtained using the RCT procedure [9, 11]. Conformational mobility and possible biochemical heterogeneity of samples were observed [9–12], and an anisotropic collapse was seen in structures as a result of air drying of the samples [9, 11].

Still, the data allowed first 3D reconstructions for the RSC complex (one of them is shown in Fig. 2a) and showed that RSC has four domains, which are arranged in a C-shaped structure. The domains surround a central cavity, and the size of the cavity is comparable with the size of a nucleosome. The structures solved at low resolution (25–40 Å) made it possible to speculate on the RSC function. Unfortunately, none of the structures showed RSC in a complex with

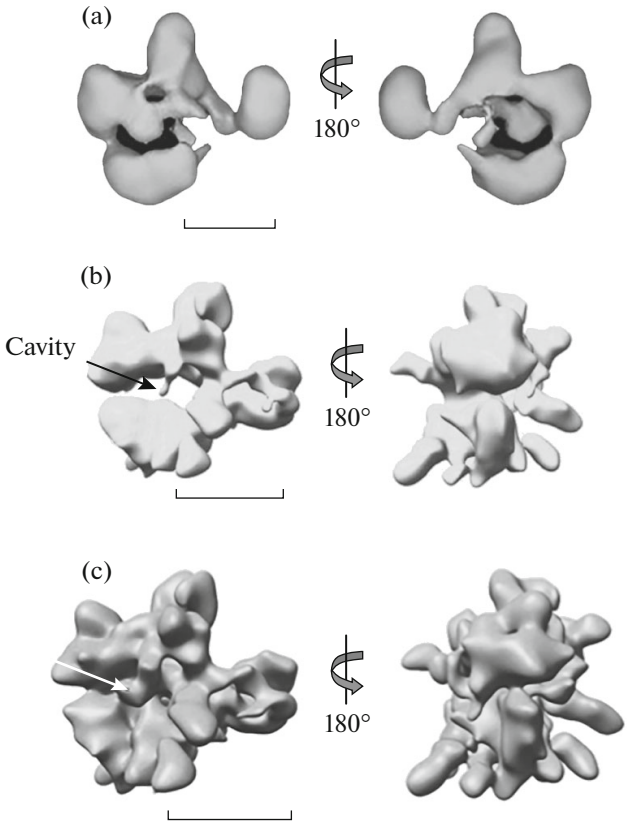

Fig. 2. RSC structure examined by negative staining and cryo-TEM. Two views, one rotated 180° about the vertical axis, are shown for each reconstruction. (a) RSC structure obtained with negative staining [9]. (b) RSC structure obtained by cryo-TEM [12]. The cavity is indicated with a black arrow. (c) 3D reconstruction of a RCS–nucleosome complex from cryo-TEM data [12]. The central cavity seen in (b) is occupied by histones (a white arrow).

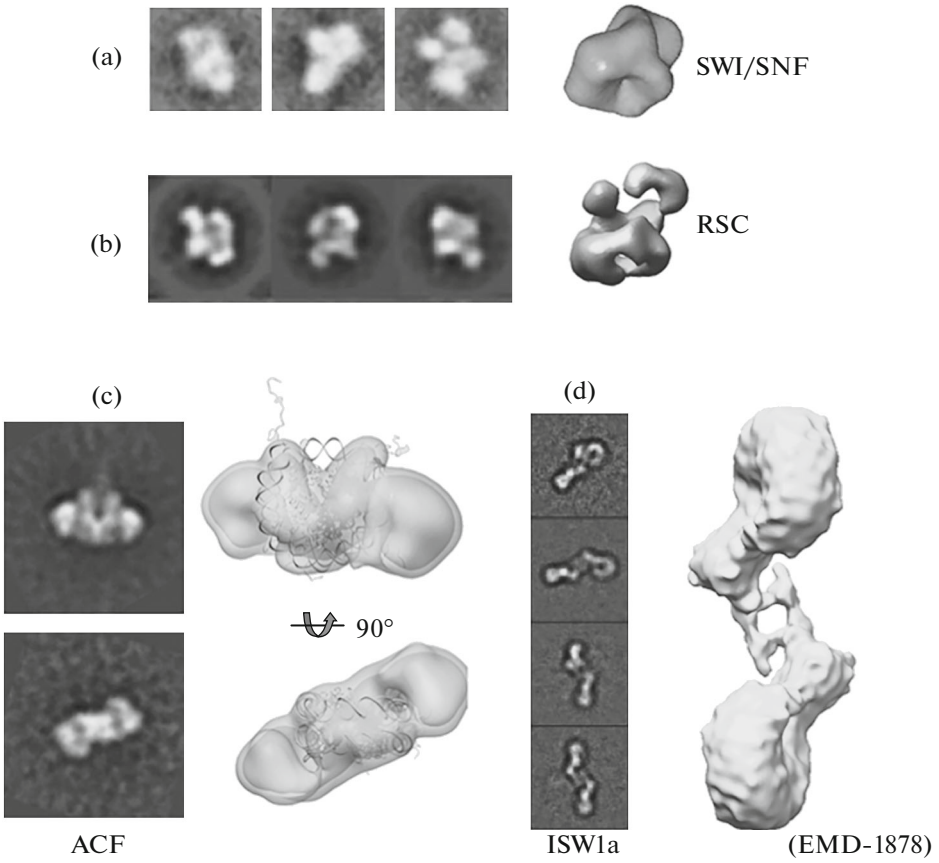

Fig. 3. Significance of symmetry factors. Projections (on the left) and a structure (on the right) are shown for each CRF. (a) SWI/SNF structure obtained using STEM [14]. (b) RSC structure obtained using RCT [10]. (c) Structure of a dimer of the ACF catalytic subunits with a nucleosome (C2 pseudosymmetry) [17]. (d) Structure of the HSS-Ioc3-45N0 (ISW1a-ΔATPase–nucleosome) with C2 symmetry [18]. The EMDB accession number is given.

a nucleosome, indicating that the complex is unstable in vitro. To interpret the reconstructions, a nucleosome structure in crystal [23] was retrieved from PDB (ID 1AOI), filtered to low resolution, and fitted in the central cavity (Figs. 4a, 4b).

Cryo-Electron Microscopy of CRFs

Cryo-electron microscopy (cryo-TEM) makes it possible to stabilize the sample in a native hydrated state. Rapid freezing is used to obtain the sample in a solid state without its dehydration or the formation of ice crystals; the sample is maintained at a low temperature during its treatment and analysis under an electron microscope. A low temperature substantially decelerates sample damage by the electron beam [21, 24, 25]. Cryo-TEM makes it possible to achieve high resolution, but images have a poor signal-to-noise ratio, which may complicate the data processing, and are prone to artifacts. To overcome these difficulties, comparisons are usually made with available negative staining data.

Only few CRF reconstructions, including SWR1 [20] and SWI/SNF [15], were obtained using cryo-TEM, and the structure of the RSC complex was refined to a resolution of approximately 25 Å [12] (Fig. 2b). Cryo-TEM images of RSC were aligned with the structure obtained for RSC with negative staining (Fig. 2a) [9]. The cryo-TEM data confirmed that the RSC complex is formed of four domains and have a central cavity fit to accommodate a nucleosome. A first reconstruction was obtained for the RSC complex with a nucleosome (Fig. 2b) [12]. For this purpose, RSC was combined with a fourfold excess of nucleosomes in vitro, and a difference map between the RSC and RSC–nucleosome structures was calculated. The difference density on the map had dimensions of a histone octamer without DNA. The finding indicates that RSC may interact with histones in the absence of DNA.

SIGNIFICANCE OF SYMMETRY FACTORS

Symmetry is important for specimens examined by TEM. Various symmetry types (crystal, helical, icosa-

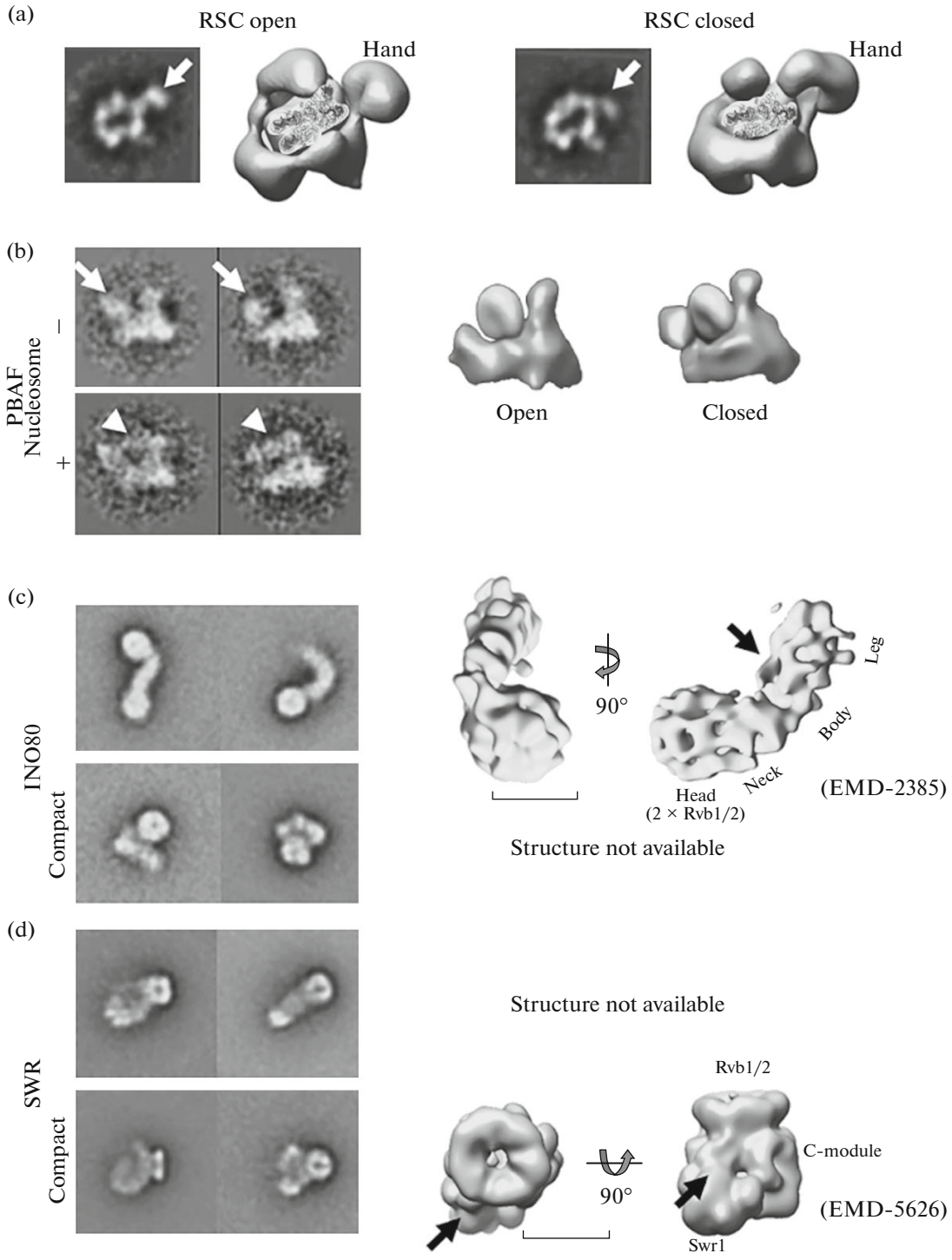

Fig. 4. Conformational mobility of CRFs. Projections (on the left) and structures (on the right) are shown in each case. (a) RSC structures in open and closed conformations [10]. Domains with different positions are indicated with arrows. (b) Interaction of PBAF with a nucleosome. The arrows indicate a cavity in the structure, triangle corners, the nucleosome [13]. (c) Structure of INO80 [29]. (d) Structure of SWR1 [29]. Black arrows indicate the possible localization of the nucleosome. The EMDB accession numbers are given.

hedral, and rotational symmetries) increase the signal-to-noise ratio of sample images and decrease the image number required for 3D reconstructions. Unfortunately, the majority of CRFs lack symmetry. This circumstance complicates their reconstruction, and possible reconstruction defects are difficult to avoid.

Asymmetric CRFs (SWI/SNF, RSC, and PBAF)

To illustrate structural diversity of asymmetric CRFs, we compared the 3D reconstructions of the yeast CRFs SWI/SNF [14] and RSC [9]. The two factors were both examined by negative staining TEM and have a high amino acid sequence similarity. Yet the 3D structures of SWI/SNF and RSC differ substantially. The SWI/SNF structure is more compact and shows a uniform electron density distribution (Fig. 3a), while RSC is shaped as a ring with domains surrounding a central cavity (Fig. 3b). It should be noted that some SWI/SNF 2D projections used in reconstruction showed a considerable similarity to RSC projections; in particular, they had four characteristic domains (Figs. 3a, 3b; left panels). It remains unclear whether the difference reflects the actual structural features of the factors, or the actual similarity was lost because different techniques (RCT and STEM) were employed in reconstruction.

On the other hand, yeast RSC [9–12] and human PBAF [13] are similar in architecture [10] (Figs. 4a, 4b) in spite of lack of amino acid sequence conservation. The structural similarity most likely reflects similar mechanisms of action [12].

Symmetric CRFs: ACF and ISW1a

Rotational symmetry or pseudosymmetry is characteristic of certain CRFs.

The reconstruction shown in Fig. 3c is a fragment of the ACF complex that includes the SNF2h catalytic ATPase subunit and the Acf1 accessory subunit. The structure was reconstructed using negative staining to 27 Å resolution. Image classification revealed three different projection type classes, each displaying 2C symmetry, which reflected the interaction of two SNF2h monomers with a nucleosome. The reconstruction was interpreted using a nucleosome structure in crystal [23]. The electron density corresponding to nucleosomal DNA was not reconstructed throughout its length, as was the case with RSC [12], indicating again that DNA is unwrapped from the histone octamer during chromatin remodeling. Two ACF motors face each other, which enables ACF to rapidly change the direction of nucleosome movement to achieve a certain distance between them. It is also known that DNA is unwrapped from the histone octamer during transcription through nucleosomes [26].

Another structure with C2 symmetry was obtained for a complex of ISW1a-(ΔATPase) with the nucleosome by cryo-TEM [18] (Fig. 3d). HSS-Ioc3 and nucleosome crystal structures were fit in the electron density resolved to 24 Å for their identification [27]. The interaction in the ISW1a-(ΔATPase)–nucleosome complex proved to be restricted to linker DNA and a DNA fragment downstream of the linker. It was found that ISW1a is capable of interacting with two linker DNA regions simultaneously. A mechanism of ISW1a-dependent nucleosome remodeling was proposed with due regard to biochemical data [18], basically differing from the mechanism utilized by ACF (see below).

CONFORMATIONAL MOBILITY OF CRFs

Conformational mobility is common for all CRFs. As a result, domains may occur in different relative orientations on 2D projections of macromolecules (Fig. 4).

For instance, RSC and PBAF have a C-shaped structure with four domains surrounding a central cavity (Figs. 4a, 4b). Electron microscopy revealed several domain positions in a nucleosome-free sample. To classify the projections, the orientation and arrangement were determined by cross-comparisons of images or comparisons with projections of a 3D model. Conformation collations and analysis showed that mobility is clearly seen for the largest right domain, the arm, of RSC (Fig. 4a, arrows) [10] and is less distinct in the lower domain [9, 11, 12]. The upper left domain is mobile in PBAF (Fig. 4b, white arrows). Open and closed conformations were assumed for RSC and PBAF based on mobility of their regions.

When mononucleosomes were added to PBAF, the portion of complexes was low (approximately 5%) in the sample [13]. A classification of complex-showing images revealed several projections with an additional electron density in the region between the mobile and immobile domains (Fig. 4b, arrowheads). However, the data were not ample enough to allow a 3D reconstruction for the PBAF–nucleosome complex.

The majority of CRFs occur in an open conformation in nucleosome-free samples. The possibility of nucleosome accommodation in the central cavty of PBAF was assessed by docking the nucleosome crystal structure (PDB 1AOI [23]) filtered to a proper resolution (20–25 Å). The nucleosome is docked into the free region bounded by the flexible CRF domains (Figs. 4a, 4b) [10, 13]. The dimensions of the RSC and PBAF central spaces agree well with the nucleosome size in both open and closed conformations, supporting the flexible arm model (see below) of chromatin remodeling [10]. A single nucleosome was identified as a preferential substrate of RSC. RSC was earlier shown to bind a nucleosome with nanomolar affinity [28] and to prevent various nucleases from affecting nucleosomal DNA [9]. Moreover, the data on nucleosome binding in the RSC or PBAF central cavity agree with the results of nuclease footprinting of nucleosomal DNA [10, 13].

Members of the SWR/INO80 family function as ATP-dependent DNA translocases and utilize the energy of ATP hydrolysis to disrupt the DNA–histone interactions when exchanging a H2A.Z/H2B dimer for H2A/H2B. Three structures are currently available for members of the family: two structures were

obtained for yeast INO80 by negative staining and cryo-TEM [19] and one structure was resolved for yeast SWR1 by cryo-negative staining TEM [20]. The structures substantially differ from each other. INO80 is an elongate molecule (Fig. 4c), while SWR1 is compact (Fig. 4d). Four subdomains are recognized in the INO80 structure, which has an embryo-shaped head–neck–body–foot architecture. To interpret the results, a Rvb1/2 dodecamer was placed into the region of the head in line with the dimensions of this domain [19].

In the compact SWR1 structure (Fig. 4d), a domain with a pseudo sixfold radial structure corresponds to the Rvb1/2 heterohexamier. The N- and C-modules and the Swr1 domain were additionally identified [20]. Thus, the structures of two members of the family (SWR and INO80) differ. According to a model supported by an analysis of projection images obtained for INO80–nucleosome complexes with negative staining, a nucleosome is accommodated in the central groove of INO80 (Fig. 4c, an arrow). The flexible foot was assumed to extend (an open state) and to bend (a closed state) in the course of chromatin remodeling [19].

To study how SWR1 binds a nucleosome, the structure of a SWR1–nucleosome complex was reconstructed at a 34 Å resolution [20]. The reconstruction was compared with the structure of apo-SWR1 (without a nucleosome), and an additional density was observed over the central depression formed between the Rvb1/Rvb2 ring and the Swr1 ATPase (Fig. 4d; the possible nucleosome position is indicated with arrows). However, the dimensions of the additional density were not large enough to dock a nucleosome, which was possibly due to conformational and biochemical heterogeneity of this CRF.

Watanabe et al. [29] showed recently that projection images of two different CRFs, INO80-C and SWR-C, are similar and suggest two, extended and compact, conformations in either sample (Figs. 4c, 4d). The observation possibly indicates that the two CRFs of the SWR/INO80 family are actually similar in structure, but their structures were reconstructed for the extended (active) conformation in the case of INO80 and the closed (compact) conformation in the case of SWR1. Members of the SWI/SNF and SWR/INO80 seem to have more structural similarities than was believed earlier [29]. There is still a substantial difference. The nucleosome is accommodated within the complex in the case of SWI/SNF members (Figs. 2c, 4a, 4b) and is on one side of the complex in the case of SWR/INO80 members (Figs. 4c, 4d). This nucleosome position destabilizes the complexes and makes it difficult to resolve their structures to a high resolution.

INTERPRETATION OF STRUCTURES

To establish the domain organization of CRFs and to hypothesize their functions, it is essential to correctly interpret their structures. The results make it possible to speculate on conformational changes in macromolecules and their interactions with ligands.

Docking of Crystal Structures

All 3D structures of CRFs were reconstructed to a resolution of 17.5–43 Å, which is too low to identify α-helices in proteins. To improve the interpretation, crystal structures of individual domains are docked into TEM maps. Crystal structures of full-size CRF complexes are not available from PDB because the complexes are conformationally labile and are impossible to obtain in crystal. Crystal structures are only available for individual domains of ISW1a [18] and INO80/SWR1: the isolated Rvb1/2 domains [30–34], the YEATS domain of Taf14 [55], and the Arp4 and Arp8 actin-binding subunits [35–37]. To interpret the INO80 structure, the Rvb1/2 dodecamer and the Snf2 domain were docked into the INO80 electron density map, and the other structural modules were related to their subcomplexes with the use of affinity labeling [18].

Affinity Labeling

The DID1 affinity label was used to localize the Arp8, Nhp10, and Arp5 modules in the INO80 complex [18, 38]. As a result, detection of an additional density corresponding to the label in a particular region made it possible to map the Arp5, Arp8, Nhp10, less2, and less6 domains in the INO80 electron density.

Crosslinking Methods

The interaction of INO80 with the nucleosome was studied using crosslinking and mass spectrometry (XL-MS) [39]. A total of 52 crosslinks were detected, including 35 within flexible histone tails and 17 between structural components of histones and INO80. The findings make it possible to approximately determine the nucleosome position (Fig. 4c, an arrow) [18]. Crosslinks with histones H2A and H2B indicated that the H2A/H2B dimer is in the neck region of INO80, providing for ATP-dependent chemomechanical activity of the Snf2 domain. It is thought that the contacts with DNA and H2A.Z/H2B and H2A/H2B histone dimers subject to exchange may be lost.

Mapping by Subtracting Electron Density

To map the domains corresponding to the C- and N-terminal modules of the SWR complex, subcomplexes devoid of the domains were synthesized and their 3D structures reconstructed. The C- and N-modules

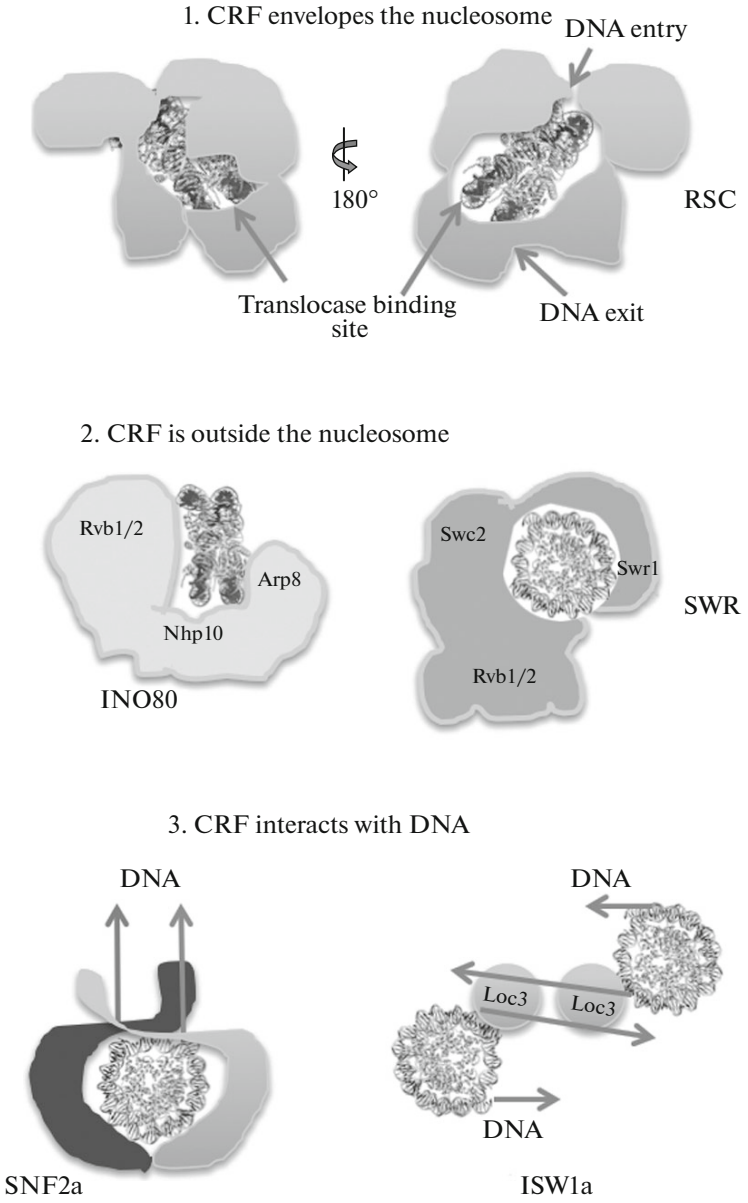

Fig. 5. Models proposed for the interactions of various CRFs with the nucleosome on the basis of structural studies. 1. RSC in a closed conformation envelopes the nucleosome. 2. The nucleosomes is not completely enveloped by INO80 or SWR. 3. A complex of the nucleosome with two SNF2h molecules (on the left) and a hypothetical model of ISW1a-driven translocation (on the right).

were localized by constructing the maps of density differences between the truncated subcomplex structures and the initial full-size SWR1 structure. The same method was used to localize the nucleosome in complexes with SWR1 [20], INO80 [18], RSC [12], and PBAF [13]. An extra electron density was seen in projections of the nucleosome-containing complexes (Fig. 4b, arrows).

Structural Data-Based Models of the CRF Function

A comparison of structures from different classes makes it possible to study their structural features in association with the functional roles of individual domains. Data obtained by different methods, including information from biochemical and biophysical studies, are considered collectively to confirm or reject the hypotheses on the functions of molecular machines, such as CRFs. Spatial structure analyses showed that interactions of CRFs with the nucleosome yield various structural complexes, which move nucleosomal DNA, play a role in histone exchange, or evenly space nucleosomes along DNA. Several hypotheses were advanced to explain the CRF functions in the course of chromatin remodeling.

1. CRF envelopes the nucleosome: A flexible arm hypothesis. The flexible arm hypothesis was advanced more than 10 years ago in a study of conformational

changes in the RSC complex [9] and received further development when several other structures were reconstructed for members of the same [12, 13, 40]. Proteins of the SWI/SNF family play a role in DNA movement along the nucleosome, nucleosome detachment (when nucleosomes are removed from intensely transcribed genes), and partial histone loss (during transcription of nucleosomal DNA). CRFs act to disrupt and to restore the contacts between histones and DNA in these processes [6, 41, 42].

The flexible arm hypothesis suggests that a CRF assumes an open conformation to interact with a nucleosome (Figs. 4a, 4b) and than changes to a closed conformation by moving one (PBAF) or several (RSC) domains. The nucleosome is thus placed within the CRF and is enveloped on two or more sides (Fig. 5). The spatial organization of the RSC and PBAF 3D structures (Figs. 4a, 4b) allows the central space to act as a nucleosome-binding site. The assumption was directly confirmed by comparing with projections of the PBAF–nucleosome complex (Fig. 4b).

It was thought earlier that ATP-dependent DNA movement around a nucleosome during remodeling involves a bending of the double helix [7, 43] and results in a large loop (more than 100 bp) [44, 45]. However, only small loops (less than 20 bp) can be accommodated in the cavity in the closed conformation. The formation of larger loops would lead to discordance, i.e., the DNA loops would not fit in the cavity, and nucleosomal DNA would be exposed to the solvent. Substantial conformational changes would otherwise be necessary for accommodating a larger loop [46]. The CRF–nucleosome interaction seems to cause partial DNA unwinding. The assumption agrees with a cryo-TEM RSC structure [12], where the electron density of nucleosomal DNA cannot be identified.

2. Localization of CRF outside the nucleosome: A histone displacement hypothesis. A mechanism assumed for the interaction of SWR/INO80 family CRFs with the nucleosome during invariant histone exchange differs from the above mechanism of the SWI/SNF function. In histone exchange [47, 48], the resident H2A/H2B dimer is displaced from the nucleosome, and a H2A.Z/H2B dimer is inserted in its place [20].

It is thought that the Rvb1/Rvb2 hexamer of SWR/INO80 CRFs acts as a structural platform to accommodate the modules that interact with various substrates (Fig. 5). The assumption is supported by a 3D map of SWR1, which preserves its structural characteristics regardless of the presence of individual modules [20]. A similar structural platform was assumed for INO80 [49] and SAGA histone acetyltransferase [50].

3. CRFs interact with DNA: A sliding hypothesis. To control the distribution of nucleosomes along DNA, CRFs interact with linker DNA or unmodified histone regions rather than with the nucleosome core [51]. The CRFs SNF2h [17] and ISW1a [18] act differently to play a role in nucleosome distribution (Fig. 5).

In the former case, there are two SN2h monomers per one nucleosome, but only one of them utilizes the ATP energy. This monomer interacts with the N end of histone H4 and the corresponding linker DNA region. A longer linker stimulates ATPase/translocase activity of SNF2h [52–55], leading to a bridging of the two SNF2h monomers. The catalytic ATPase subunit Swi/Snf2 disrupts the DNA–histone interactions [55, 56] and generates either superhelical DNA twist [57] or a running DNA bulge [58]. The process yields nucleosomes having equally sized linkers on both sides (Fig. 5).

The ISW1a complex binds to the linker DNA region that is subject to translocation. Once the linker reached a necessary length, ISW1a blocks further translocation.

CONCLUSIONS

Elucidation of the mechanisms underlying the CRF function is still in its infancy. To achieve a resolution better than 6 Å in reconstructions, far more images of single particles are required for structures lacking symmetry than for structures with symmetry. Conformational mobility complicates the reconstruction because greater data sets should be processed to separate the structures with different conformations. The problem is solved with modern cryo-electron microscopes, which allow automated data collection and produce millions of single-particle images in a few hours. In addition, current image processing methods and supercomputers make it possible to process large data sets to obtain 3D reconstructions at nearly atomic resolution. However, the interpretation of different conformations requires that the relevant hypotheses are verified using biochemical methods.

ACKNOWLEDGMENTS

This work was supported by the Russian Science Foundation (project no. 14-24-00031).

REFERENCES

1. Clapier C.R., Cairns B.R. 2009. The biology of chromatin remodeling complexes. *Annu. Rev. Biochem.* **78**, 273–304.
2. Vignali M., Hassan A.H., Neely K.E., Workman J.L. 2000. ATP-dependent chromatin-remodeling complexes. *Mol. Cell. Biol.* **20**, 1899–1910.
3. Lai A.Y., Wade P.A. 2011. Cancer biology and NuRD: A multifaceted chromatin remodeling complex. *Nat. Rev. Cancer.* **11**, 588–596.
4. Conaway R.C., Conaway J.W. 2009. The INO80 chromatin remodeling complex in transcription, replication and repair. *Trends Biochem. Sci.* **34**, 71–77.

5. Yen K., Vinayachandran V., Pugh B.F. 2013. SWR-C and INO80 chromatin remodelers recognize nucleosome-free regions near +1 nucleosomes. *Cell.* **154**, 1246–1256.
6. Becker P.B., Horz W. 2002. ATP-dependent nucleosome remodeling. *Annu. Rev. Biochem.* **71**, 247–273.
7. Saha A., Wittmeyer J., Cairns B.R. 2006. Chromatin remodelling: The industrial revolution of DNA around histones. *Nat. Rev. Mol. Cell Biol.* **7**, 437–447
8. Gangaraju V.K., Bartholomew B. 2007. Mechanisms of ATP dependent chromatin remodeling. *Mutat. Res.* **618**, 3–17.
9. Asturias F.J., Chung W.H., Kornberg R.D., Lorch Y. 2002. Structural analysis of the RSC chromatin-remodeling complex. *Proc. Natl. Acad. Sci. U. S. A.* **99**, 13477–13480.
10. Leschziner A.E., Saha A., Wittmeyer J., Zhang Y., Bustamante C., Cairns B.R., Nogales E. 2007. Conformational flexibility in the chromatin remodeler RSC observed by electron microscopy and the orthogonal tilt reconstruction method. *Proc. Natl. Acad. Sci. U. S. A.* **104**, 4913-4918.
11. Skiniotis G., Moazed D., Walz T. 2007. Acetylated histone tail peptides induce structural rearrangements in the RSC chromatin remodeling complex. *J. Biol. Chem.* **282**, 20804–20808.
12. Chaban Y., Ezeokonkwo C., Chung W.H., Zhang F., Kornberg R.D., Maier-Davis B., Lorch Y., Asturias F.J. 2008. Structure of a RSC–nucleosome complex and insights into chromatin remodeling. *Nat. Struct. Mol. Biol.* **15**, 1272–1277.
13. Leschziner A.E., Lemon B., Tjian R., Nogales E. 2005. Structural studies of the human PBAF chromatin-remodeling complex. *Structure*. **13**, 267–275.
14. Smith C.L., Horowitz-Scherer R., Flanagan J.F., Woodcock C.L., Peterson C.L. 2003. Structural analysis of the yeast SWI/SNF chromatin remodeling complex. *Nat. Struct. Biol.* **10**, 141–145.
15. Dechassa M.L., Zhang B., Horowitz-Scherer R., Persinger J., Woodcock C.L., Peterson C.L., Bartholomew B. 2008. Architecture of the SWI/SNF-nucleosome complex. *Mol. Cell. Biol.* **28** (19), 6010–6021.
16. Hu M., Zhang Y.B., Qian L., Brinas R.P., Kuznetsova L., Hainfeld J.F. 2008. Three-dimensional structure of human chromatin accessibility complex hCHRAC by electron microscopy. *J. Struct. Biol.* **164**, 263–269.
17. Racki L.R., Yang J.G., Naber N., Partensky P.D., Acevedo A., Purcell T.J., Cooke R., Cheng Y., Narlikar G.J. 2009. The chromatin remodeller ACF acts as a dimeric motor to space nucleosomes. *Nature.* **462**, 1016–1021.
18. Yamada K., Frouws T.D., Angst B., Fitzgerald D.J., DeLuca C., Schimmele K., Sargent D.F., Richmond T.J. 2011. Structure and mechanism of the chromatin remodelling factor ISW1a. *Nature*. **472**, 448–453.
19. Tosi A., Haas C., Herzog F., Gilmozzi A., Berninghausen O., Ungewickell C., Gerhold C.B., Lakomek K., Aebersold R., Beckmann R., Hopfner K.-P. 2013. Structure and subunit topology of the INO80 chromatin remodeler and its nucleosome complex. *Cell.* **154**, 1207–1219.
20. Nguyen Q.V., Ranjan A., Stengel F., Wei D., Aebersold R., Wu C., Leschziner A.E. 2013. Molecular architecture of the ATP-dependent chromatin-remodeling complex SWR1. *Cell*. **154**, 1220–1231.
21. Orlova E., Saibil H. 2011. Structural analysis of macromolecular assemblies by electron microscopy. *Chem. Rev*. **111**, 7710–7748.
22. Sherman M.B., Orlova E.V., Terzyan S.S., Kleine R., Kiselev N.A. 1981. On the negative straining of the protein crystal structure. *Ultramicroscopy*. **7** (2), 131–138.
23. Luger K., Mäder A.W., Richmond R.K., Sargent D.F., Richmond T.J. 1997. Crystal structure of the nucleosome core particle at 2.8 Å resolution. *Nature*. **6648**, 251–260.
24. Dubochet J., Adrian M., Chang J.J., Homo J.C., Lepault J., McDowall A.W., Schultz P. 1988. Cryo-electron microscopy of vitrified specimens. *Q. Rev. Biophys.* **2**, 129–228.
25. Dobro M.J., Melanson L.A., Jensen G.J., McDowall A.W. 2010. Plunge freezing for electron cryomicroscopy. *Methods Enzymol*. **481**, 63–82.
26. Gaykalova D., Kulaeva O., Volokh O., Shaytan A., Fu-Kai Hsieh, Kirpichnikov M., Sokolova O., Studitsky V. 2015. Structural analysis of nucleosomal barrier to transcription. www.pnas.org/cgi/doi/10.1073/pnas.1508371112.
27. Davey C.A., Sargent D.F., Luger K., Ma¨der A.W., Richmond T.J. 2002. Solvent mediated interactions in the structure of the nucleosome core particle at 1.9 Å resolution. *J. Mol. Biol.* **319**, 1097–1113.
28. Lorch Y., Cairns B.R., Zhang M., Kornberg R.D. 1998. Activated RSC-nucleosome complex and persistently altered form of the nucleosome. *Cell.* **94**, 29–34.
29. Watanabe S., Tan D., Lakshminarasimhan M., Washburn M.P., Hong E.J., Walz T., Peterson C.L. 2015. Structural analyses of the chromatin remodelling enzymes INO80-C an SWR-C. *Nat. Commun*. **6**, 7108.
30. Gorynia S., Bandeiras T.M., Pinho F.G., McVey C.E., Vonrhein C., Round A., Svergun D.I., Donner P., Matias P.M., Carrondo M.A. 2011. Structural and functional insights into a dodecameric molecular machine: The RuvBL1/RuvBL2 complex. *J. Struct. Biol.* **176**, 279–291.
31. Lopez-Perrote A., Munoz-Hernandez H., Gil D., Llorca O. 2012. Conformational transitions regulate the exposure of a DNA-binding domain in the RuvBL1–RuvBL2 complex. *Nucleic Acids Res.* **40**, 11086–11099.
32. Matias P.M., Gorynia S., Donner P., Carrondo M.A. 2006. Crystal structure of the human AAA+ protein RuvBL1. *J. Biol. Chem*. **281**, 38918–38929.
33. Puri T., Wendler P., Sigala B., Saibil H., Tsaneva I.R. 2007. Dodecameric structure and ATPase activity of the human TIP48/TIP49 complex. *J. Mol. Biol.* **366**, 179–192.
34. Torreira E., Jha S., Lopez-Blanco J.R., Arias-Palomo E., Chacon P., Canas C., Ayora S., Dutta A., Llorca O. 2008. Architecture of the pontin/reptin complex, essential in the assembly of several macromolecular complexes. *Structure.* **16**, 1511–1520.
35. Fenn S., Breitsprecher D., Gerhold C.B., Witte G., Faix J., Hopfner K.P. 2011. Structural biochemistry of nuclear actin-related proteins 4 and 8 reveals their interaction with actin. *EMBO J.* **30**, 2153–2166.
36. Gerhold C.B., Winkler D.D., Lakomek K., Seifert F.U., Fenn S., Kessler B., Witte G., Luger K., Hopfner K.P.

2012. Structure of actin-related protein 8 and its contribution to nucleosome binding. *Nucleic Acids Res.* **40**, 11036–11046.

37. Saravanan M., Wuerges J., Bose D., McCormack E.A., Cook N.J., Zhang X., Wigley D.B. 2012. Interactions between the nucleosome histone core and Arp8 in the INO80 chromatin remodeling complex. *Proc. Natl. Acad. Sci. U. S. A.* **109**, 20883–20888.

38. Flemming D., Thierbach K., Stelter P., Böttcher B., Hurt E. 2010. Precise mapping of subunits in multiprotein complexes by a versatile electron microscopy label. *Nat. Struct. Mol. Biol.* **17**, 775–778.

39. Herzog F., Kahraman A., Boehringer D., Mak R., Bracher A., Walzthoeni T., Leitner A., Beck M., Hartl F.U., Ban N., Malmstrom L., Aebersold R. 2012. Structural probing of a protein phosphatase 2A network by chemical cross-linking and mass spectrometry. *Science.* **337**, 1348–1352.

40. Leschziner A.E. 2011. Electron microscopy studies of nucleosome remodelers. *Curr. Opin. Struct. Biol.* **6**, 709–718.

41. Flaus A., Owen-Hughes T. 2001. Mechanisms for ATP- dependent chromatin remodelling. *Curr. Opin. Genet. Dev.* **11**, 148–154.

42. Narlikar G.J., Fan H.Y., Kingston R.E. 2002. Cooperation between complexes that regulate chromatin structure and transcription. *Cell.* **108**, 475–487.

43. Lorch Y., Davis B., Kornberg R.D. 2005. Chromatin remodeling by DNA bending, not twisting. *Proc. Natl. Acad. Sci. U. S. A.* **102**, 1329–1332.

44. Zofall M., Persinger J., Kassabov S.R., Bartholomew B. 2006. Chromatin remodeling by ISW2 and SWI/SNF requires DNA translocation inside the nucleosome. *Nat. Struct. Mol. Biol.* **13**, 339–346.

45. Lia, G., Praly, E., Ferreira, H., Stockdale, C., Tse-Dinh, Y. C., Dunlap, D., Croquette V., Bensimon D., Owen-Hughes T. 2006. Direct observation of DNA distortion by the RSC complex. *Mol. Cell.* **21**, 417–425.

46. Tanga L., Nogales E., Ciferrie C. 2010. Structure and function of SWI/SNF chromatin remodeling complexes and mechanistic implications for transcription. *Progr. Biophys. Mol. Biol.* **102,** 122–128.

47. Luk E., Ranjan A., Fitzgerald P.C., Mizuguchi G., Huang Y., Wei D., Wu C. 2010. Stepwise histone replacement by SWR1 requires dual activation with histone H2A.Z and canonical nucleosome. *Cell.* **143**, 725–736.

48. Mizuguchi G., Shen X., Landry J., Wu W.-H., Sen S., Wu C. 2004. ATP-driven exchange of histone H2AZ variant catalyzed by SWR1 chromatin remodeling complex. *Science.* **303**, 343–348.

49. Kapoor P., Chen M., Winkler D.D., Luger K., Shen X. 2013. Evidence for monomeric actin function in INO80 chromatin remodeling. *Nat. Struct. Mol. Biol.* **20**, 426–432.

50. Chittuluru J.R., Chaban Y., Monnet-Saksouk J., Carrozza M.J., Sapountzi V., Selleck W., Huang J., Utley R.T., Cramet M., Allard S., Cai G., Workman J.L., Fried M.G., Tan S., Côté J., Asturias F.J. 2011. Structure and nucleosome interaction of the yeast NuA4 and Piccolo–NuA4 histone acetyltransferase complexes. *Nat. Struct. Mol. Biol.* **18**, 1196–1203.

51. Boyer L.A., Latek R.R., Peterson C.L. 2004. The SANT domain: A unique histone-tail-binding module? *Nat. Rev. Mol. Cell Biol.* **5**, 158–163.

52. Stockdale C., Flaus A., Ferreira H., Owen-Hughes T. 2006. Analysis of nucleosome repositioning by yeast ISWI and Chd1 chromatin remodeling complexes. *J. Biol. Chem.* **281**, 16279–16288.

53. Whitehouse I., Stockdale C., Flaus A., Szczelkun M.D., Owen-Hughes T. 2003. Evidence for DNA translocation by the ISWI chromatin-remodeling enzyme. *Mol. Cell. Biol.* **23**, 1935–1945.

54. Yang J.G., Madrid T.S., Sevastopoulos E., Narlikar G.J. 2006. The chromatin-remodeling enzyme ACF is an ATP-dependent DNA length sensor that regulates nucleosome spacing. *Nat. Struct. Mol. Biol.* **13**, 1078–1083.

55. Zofall M., Persinger J., Kassabov S.R., Bartholomew B. 2006. Chromatin remodeling by ISW2 and SWI/SNF requires DNA translocation inside the nucleosome. *Nat. Struct. Mol. Biol.* **13**, 339–346.

56. Schwanbeck R., Xiao H., Wu C. 2004. Spatial contacts and nucleosome step movements induced by the NURF chromatin remodeling complex. *J. Biol. Chem.* **279**, 39933–39941.

57. Havas K., Flaus A., Phelan M., Kingston R., Wade P.A., Lilley D.M., Owen-Hughes T., 2000. Generation of super-helical torsion by ATP-dependent chromatin remodeling activities. *Cell.* **103**, 1133–1142.

58. Langst G., Becker P.B. 2001. ISWI induces nucleosome sliding on nicked DNA. *Mol. Cell.* **8**, 1085–1092.

Translated by T. Tkacheva